BRAIN RESEARCH 1190 (2008) 105–114

available at www.sciencedirect.com

ScienceDirect

www.elsevier.com/locate/brainres

BRAIN RESEARCH

Research Report

Acoustic modulation of immediate early gene expression in the auditory midbrain of female túngara frogs

Sabrina S. Burmeister, Lisa A. Mangiamele, Christina L. Lebonville*

Department of Biology, University of North Carolina, 100 South Rd., Chapel Hill, NC 27599-3280, USA

ARTICLE INFO

Article history:
Accepted 6 November 2007
Available online 12 November 2007

Keywords:
Acoustic communication
Torus semicircularis
Physalaemus pustulosus
egr-1
zenk
fos

ABSTRACT

To better understand the molecular consequences of auditory processing in frogs, we investigated the acoustic modulation of two immediate early genes (IEGs), *egr-1* and *fos*, in the auditory midbrain of female túngara frogs. Since túngara frog *egr-1* had already been identified, we first isolated a túngara-specific *fos* clone using degenerate PCR followed by Rapid Amplification of cDNA Ends. In order to examine the temporal kinetics of acoustically modulated IEG mRNA expression, we first acoustically isolated females collected from a mating chorus and analyzed the decline in IEG expression in the torus semicircularis (homolog of the inferior colliculus). We found that IEG mRNA levels declined rapidly and reached baseline within 2 h. Next, we presented females with a 30-min recording of a mating chorus and analyzed IEG expression following different survival times. We found that IEG expression increased within 15–30 min of sound presentation but, compared to other vertebrates, in the túngara frog it took longer to reach the highest and lowest mRNA levels in response to sound and isolation, respectively. We also found that acoustic stimulation of *egr-1* and *fos* differed in the three subdivisions of the torus semicircularis, suggesting that, as in birds, the two genes could provide largely different information when used in IEG mapping studies. While our results confirm the generality of sensory-induced IEG expression in vertebrates, whether the longer time course of IEG expression that we observed represents a species difference in the mechanisms of IEG transcription awaits further study.

1. Introduction

Studies of animal communication have been critical to our understanding of the neural mechanisms of sensory processing. Communication in anurans (frogs and toads) has been particularly important in studies of the evolution of behavior and its sensory mechanisms (Gerhardt and Huber, 2002). For example, research on the túngara frog (*Physalaemus pustulosus*) and its close relatives has focused intensively on female preferences for male signals as a model for understanding the evolution of communication (Ryan, 2005). Like many anurans, male túngara frogs produce mating calls that females use to locate and choose among males. Previous studies have demonstrated that the inner ear of túngara frogs is tuned to the dominant frequencies of the mating call (Wilczynski et al., 2001), but relatively little is known about auditory responses of the brains of female túngara frogs to mating calls. To begin to address this gap, in the present study, we examined acoustically

* *Corresponding author.*
E-mail address: sburmeister@unc.edu (S.S. Burmeister).
URL: http://www.bio.unc.edu/Faculty/burmeister/ (S.S. Burmeister).

0006-8993/$ – see front matter © 2007 Elsevier B.V. All rights reserved.
doi:10.1016/j.brainres.2007.11.008

modulated gene expression in three subdivisions of the torus semicircularis (homolog to the inferior colliculus) in the female túngara frog. Specifically, we examined mRNA expression of two genes, *egr-1* and *fos*, that are regulated by synaptic activity. In addition, because mate choice in frogs is manifest as acoustically guided locomotion, we explored whether gene expression in the torus semicircularis was related to variation in locomotor responses to the acoustic stimulus. Finally, an additional goal of the study was to determine the kinetics of acoustically modulated gene expression in female túngara frogs to set the stage for future studies using neural activity-dependent gene expression.

The genes *egr-1* (also known as *zenk*, *zif268*, *NGFI-A*, and *krox-24*) and *fos* code for transcription factors, and they belong to a general category of genes often called immediate early genes (IEGs). Although there are many IEGs that have a variety of functions within a cell, the role of inducible transcription factors can be generally described as linking membrane depolarization to expression of late response target genes that directly influence neuronal function (Clayton, 2000; Mello, 2004). IEG expression is linked to the activity of excitatory postsynaptic receptors by second messenger cascades (Clayton, 2000; Velho et al., 2005). One emerging view of IEG regulation is that IEG expression is promoted by increases in firing rate of presynaptic cells onto target neurons (Jarvis, 2004). Thus, when IEG mRNA or protein accumulates in neurons, we infer that they were recipients of increased presynaptic activity. However, although IEG expression apparently depends upon membrane depolarization, not all depolarization events will lead to IEG induction, which is modified by context (Jarvis et al., 1998) and experience (Mello et al., 1995; Sockman et al., 2002), and not all IEG responses will necessarily be accompanied by the production of action potentials, since the two phenomena can be experimentally decoupled (Keefe and Gerfen, 1999).

To our knowledge, a time course of sensory-induced expression of *egr-1* and *fos* has only been described in zebra finches (Mello and Clayton, 1994; Velho et al., 2005) and rats (Zangenehpour and Chaudhuri, 2002), although time courses have been reported in response to a variety of other types of stimuli (e.g., kainic acid, Burmeister and Fernald, 2005; stress, Honkaniemi et al., 1994; brain injury, Honkaniemi et al., 1995; methamphetamines, Thiriet et al., 2001). In both zebra finches and rats, sensory stimulation results in peak levels of *egr-1* and *fos* mRNA in the telencephalon after 30 min (Velho et al., 2005; Zangenehpour and Chaudhuri, 2002). Although the similarities between the zebra finches and rats suggest an evolutionary conservation of the time to peak mRNA levels for *egr-1* and *fos*, it is not clear whether this conservation extends beyond the limited number of species studied. As part of our broader effort to understand auditory physiology of female túngara frogs within a mate-choice context, a goal of the present study was to characterize the kinetics of IEG expression in response to acoustic stimulation in female túngara frogs. We focused on *egr-1* and *fos* because they are well characterized in birds and mammals and because previous studies have demonstrated acoustically modulated *egr-1* expression in brains of male (Hoke et al., 2004; Hoke et al., 2007) and female (Hoke et al., 2005) túngara frogs. Therefore, after identifying the *P. pustulosus fos* cDNA, we measured mRNA levels of *egr-1* and *fos* in the auditory midbrain in response to acoustic isolation and acoustic stimulation. We focused our measurements on three subdivisions of the midbrain torus semicircularis, the principal, laminar, and magnocellular nuclei (Fig. 1; Potter, 1965). The three nuclei are known to have distinct neuroanatomical connections (Endepols and Walkowiak, 2001; Feng and Lin, 1991), and are, collectively, the first nuclei within the frog ascending auditory system known to possess complex feature detection (Hall, 1994). Recently, it has been proposed that the laminar and magnocellular nuclei are important components of sensory-motor integration in frogs (Endepols and Walkowiak, 2001). Therefore, we also examined the relationship between acoustically induced locomotion and IEG expression in the torus semicircularis (sometimes abbreviated as torus).

2. Results

2.1. *Isolation of túngara-specific egr-1 and fos probes*

At the start of the study, our *P. pustulosus*-specific *egr-1* cDNA subclone had been previously reported (GenBank No. AY562993; Hoke et al., 2004). However, as no sequence analysis was included in that earlier study, we first examined the similarity of our *egr-1* sequence to that of other vertebrates. We found that the 411-nucleotide subclone codes for 136

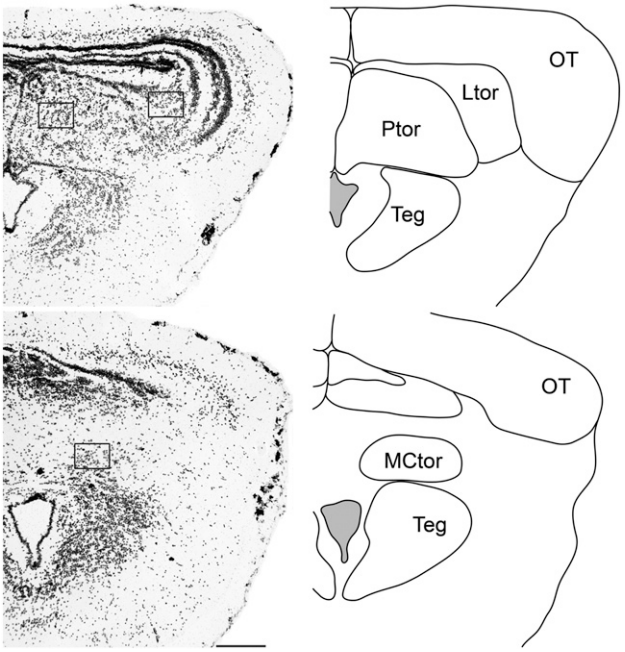

Fig. 1 – Photomicrographs and schematic diagrams of transverse hemi-sections showing sampling windows (rectangles) for the principal, laminar, and magnocellular nuclei of the torus semicircularis. Section orientation: lateral is to the right and dorsal is to the top. Scale bar represents 200 μm. Abbreviations: OT, optic tectum; Teg, tegmentum; Ltor, laminar nucleus of the torus semicircularis; MCtor, magnocellular nucleus of the torus semicircularis; Ptor, principal nucleus of the torus semicircularis.

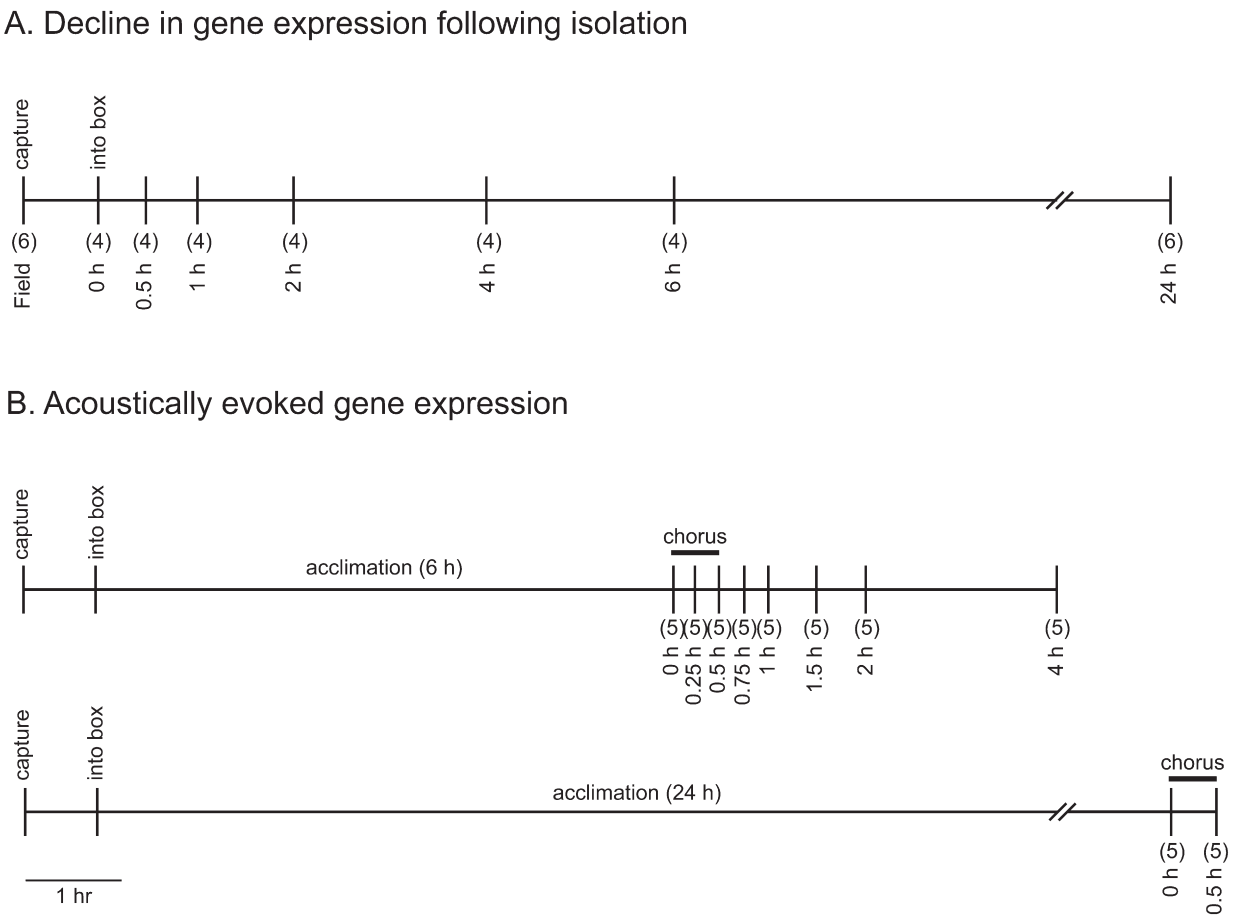

Fig. 2 – Time line of experimental treatments. (A) To investigate the decline in gene expression following acoustic isolation, we caught females in the field and transported them back to the laboratory where they were housed in sound attenuation chambers in silence. We sacrificed females in the field or after different amounts of time in the chambers; sample sizes for each group are shown in parentheses. (B) To investigate acoustically evoked gene expression, we caught females in the field, transported them back to the laboratory, and acclimated them in sound attenuation chambers for 6 or 24 h followed by presentation with a 30-min recording of a mating chorus. We sacrificed females after different amounts of time following onset of the chorus; sample sizes for each group are shown in parentheses.

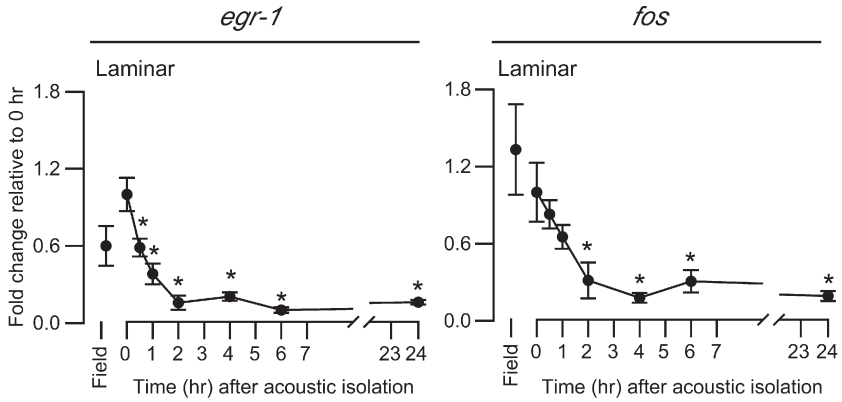

Fig. 3 – Decline in *egr-1* and *fos* mRNA expression in the laminar nucleus of the torus semicircularis in response to acoustic isolation, and, for comparison, while at the breeding ponds (field). Data are shown as mean (±SE) fold change in silver grains per cell relative to the 0-h group. All groups had a sample size of 4 except for the 24-h and field-sacrificed groups, which had a sample size of 6. Asterisks indicate groups significantly different from 0 h.

amino acids that include highly conserved regions, such as the DNA-binding domain and the first zinc finger, of the egr-1 protein. In addition, we found that the *P. pustulosus* egr-1 predicted amino acid sequence corresponded to residues 218 … 351 of *Xenopus tropicalis* egr-1 (GenBank accession no. NP_001090830). In addition, our *P. pustulosus* sequence shared 91%, 85%, and 87% identity at the amino acid level, and 86%, 76%, and 74% identity at the nucleotide level with *X. tropicalis*, chicken, and mouse egr-1 sequences, respectively. This sequence similarity supports the conclusion that our subclone corresponds to *P. pustulosus egr-1*.

To identify the *P. pustulosus fos* sequence, we used degenerate PCR followed by Rapid Amplification of cDNA Ends (RACE). We determined that the full-length transcript for *P. pustulosus fos* was 2109 nucleotides (GenBank accession no. EF566828) that code for a predicted 368-amino-acid protein (coding region 60 … 1163). The predicted amino acid sequence of our *fos* contig aligned with residues 1 … 368 of *X. tropicalis* fos (GenBank accession no. NP_001016200). In addition, the inferred coding region of our *P. pustulosus* sequence shared 85%, 64%, and 63% identity at the amino acid level, and 78%, 72%, and 79% identity at the nucleotide level with *X. tropicalis*, chicken, and mouse sequences, respectively. This sequence similarity supports the conclusion that our clone corresponds to *P. pustulosus fos*.

2.2. *Decline in gene expression following isolation*

In order to examine the temporal kinetics of sensory-induced IEG mRNA expression, we began by measuring the decline in IEG mRNA expression in the laminar nucleus of the torus (Fig. 1) in response to acoustic isolation after collection at breeding choruses (Fig. 2). Relative mRNA levels of both IEGs declined following acoustic isolation ($F_{6,24}=46.5$, $p<0.001$; Fig. 3), and the effect of isolation differed with gene (gene×isolation time: $F_{6,24}=6.5$, $p<0.001$). Both *egr-1* and *fos*

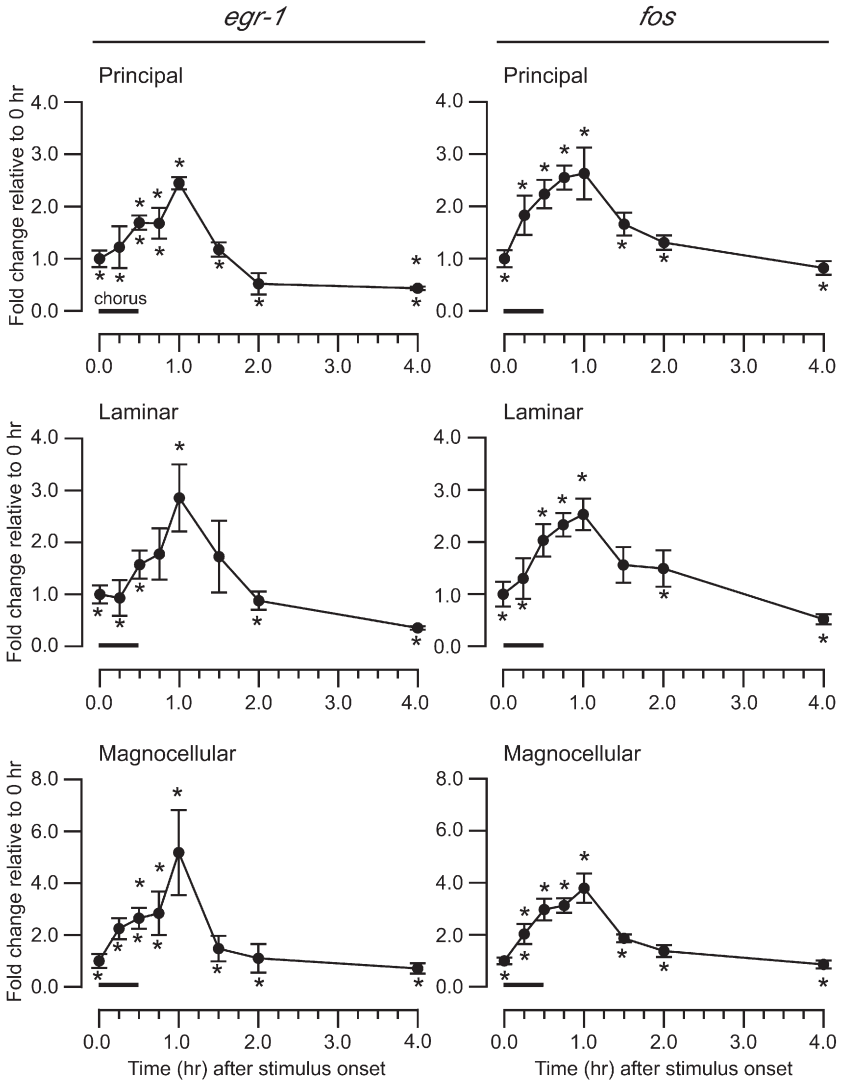

Fig. 4 – Temporal changes in *egr-1* and *fos* mRNA expression in three subdivisions of the torus semicircularis in response to a mating chorus (indicated by bar). Data are shown as mean (±SE) fold change in silver grains per cell relative to the 0-h group. Sample sizes were 5 for each group. Asterisks above symbols indicate groups that are significantly different from 0 h, and asterisks below symbols indicate groups that are significantly different from 1 h.

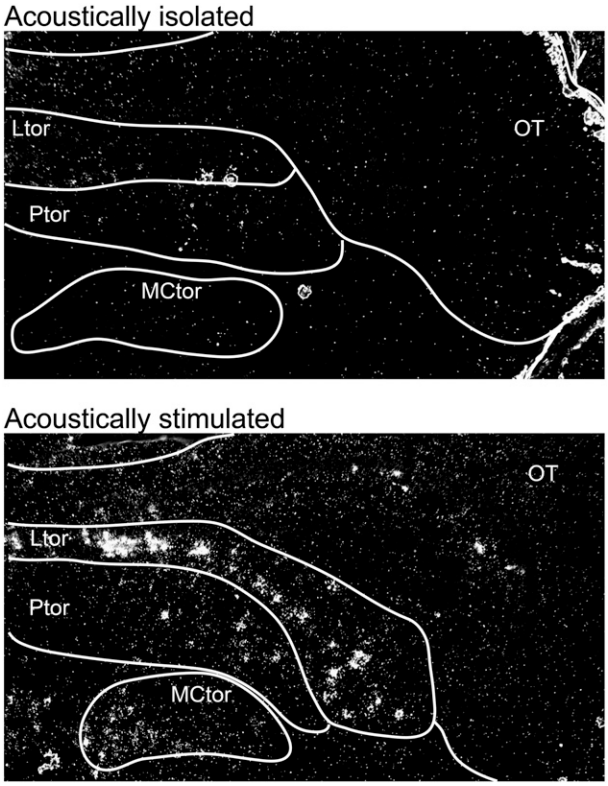

Fig. 5 – Darkfield images of radioactively labeled *fos* mRNA in the caudal region of the torus semicircularis of an acoustically isolated (0-h group) and an acoustically stimulated (1-h group) female. Boundaries of the principal (Ptor), laminar (Ltor), and magnocellular (MCtor) nuclei are shown for clarity.

reached stable low levels of mRNA expression after 2 h of isolation although *egr-1* appears to change more than *fos* within the first 2 h; after 2 h of isolation, *egr-1* levels were 16% and *fos* levels were 31% of mRNA levels before isolation. This apparent difference in mRNA decline between *egr-1* and *fos* may be due to the slightly higher starting point for *egr-1* at the 0-h time point because, when compared to mRNA levels in the field, the levels of *egr-1* (26%) and *fos* (24%) were similar after 2 h of isolation. The elevated *egr-1* levels at 0 h may indicate that *egr-1* expression in the laminar nucleus was influenced by capture and handling. Thus, we looked for a potential effect of handling by comparing *egr-1* in the field to the 0-h time point. Although we only found a weak effect of handling on *egr-1* expression ($F_{1,9}=3.8$, $p=0.085$), the issue may warrant future attention, particularly in light of the effects of restraint on the specificity of the acoustically induced *egr-1* response in zebra finches (Park and Clayton, 2002).

2.3. *Acoustically evoked gene expression*

Because sensory-induced expression of *egr-1* and/or *fos* mRNA peaks 30 min following onset of stimulation in zebra finches and rats, we designed our experiment to detect peak expression near 30 min following 6 h of acclimation in the acoustic chamber (Fig. 2). In addition, we included a subset of treatments after 24 h of acclimation (Fig. 2) to determine if acclimation period influenced the level of acoustically activated gene expression, but we found no evidence that acclimation period did so (acclimation period × survival time, all $p>0.15$). We also extended our analysis to include all three nuclei of the torus (Fig. 1).

In response to a 30-min recording of a mating chorus, both *egr-1* and *fos* mRNA increased within 15–30 min of stimulus onset and accumulation of mRNA was highest at 1 h for both genes (Fig. 4). Fig. 5 shows an example of acoustically induced IEG mRNA expression in the torus. Following the peak at 1 h, mRNA levels declined rapidly and typically reached unstimulated levels 30 to 60 min later (1.0–1.5 h after stimulus offset). Our full ANOVA model (including survival time, gene, brain region, acclimation period, and all interactions) supports an effect of survival time ($F_{1,39}=21.1$, $p<0.001$) that is similar for *egr-1* and *fos* (time × gene: $F_{7,39}=0.98$, $p=0.46$). However, there was a three-way interaction between time, brain region and gene ($F_{14,78}=2.6$, $p=0.004$), suggesting that anatomical variation in the temporal change in mRNA differed between genes. This interaction of survival time with other factors could be a product of any aspect of the temporal pattern of gene

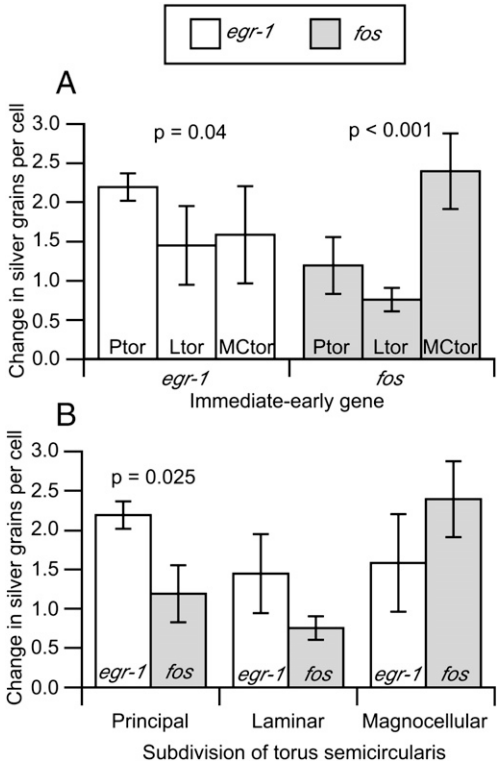

Fig. 6 – Spatial variation in acoustic stimulation of *egr-1* and *fos* mRNA expression in three subdivisions of the torus semicircularis measured 1 h after onset of a 30-min mating chorus. Data are shown as the mean (± SE) difference between 1-h and 0-h groups. Data are organized to show variation among brain regions for each gene (A) or to show variation between genes for each brain region (B). Abbreviations: OT, optic tectum; Teg, tegmentum; Ltor, laminar nucleus of the torus semicircularis; MCtor, magnocellular nucleus of the torus semicircularis; Ptor, principal nucleus of the torus semicircularis.

expression that we measured (e.g., the time of decline following peak). Since our primary interest in this experiment was the acoustically induced increase in IEGs, we repeated the ANOVA using animals only in the 0- and 1-h groups. Repeating the ANOVA with only these groups, we again found a significant three-way interaction (survival time × gene × region: $F_{2,24}=8.4$, $p=0.002$), prompting us to explore this complex interaction further.

We followed up this three-way interaction by addressing two questions. First, considering one gene at a time, we asked whether the effect of acoustic stimulation at 1 h compared to 0 h was similar among brain regions. For both *egr-1* and *fos*, the effect of acoustic stimulation differed among the three subdivisions of the torus (survival time × region, *egr-1*: $F_{2,24}=3.7$, $p=0.04$; *fos*: $F_{2,24}=14.2$, $p<0.001$). In the case of *egr-1*, the increase in mRNA was greatest for the principal nucleus whereas the acoustic induction of *egr-1* mRNA in the laminar and magnocellular nuclei was lower in comparison (Fig. 6A). For *fos*, the increase in mRNA was greatest in the magnocellular nucleus, followed by the principal and the laminar nuclei (Fig. 6A). Next, we asked whether the effect of survival time was similar for each gene within each brain region. We found that the induction pattern for the two genes differed in the principal nucleus (survival time × gene: $F_{1,12}=6.5$, $p=0.025$) where the increase in mRNA was greater for *egr-1* than *fos* (Fig. 6B). In the laminar and magnocellular nuclei, acoustic stimulation had a similar effect on *egr-1* and *fos* mRNA (Fig. 6B). We also examined the data for covariation between *egr-1* and *fos* within each brain region among stimulated animals only (1-h group) and found no evidence of a correlation (all $p>0.36$), further supporting the conclusion that, although *egr-1* and *fos* are both induced by sound in the torus, their expression patterns are distinct within and among brain regions.

In order to examine the relationship between acoustically induced behavioral responses and IEG mRNA expression, we quantified the behavior of females during the last 30 min before we collected their brains. Since females respond to the mating calls of males by moving toward the calls (females do not call), we quantified behavior by measuring the number of hops produced per minute. Females increased their motor responses during the mating chorus (Fig. 7; $F_{5,28}=7.8$, $p<0.001$), and acclimation period had a significant influence on this response (acclimation period × time: $F_{1,28}=8.0$, $p=0.008$). Females in the 6-h acclimation period typically oriented toward the speaker and hopped actively during the playback and they otherwise remained comparatively still. In contrast, females who were acclimated for 24 h in the acoustic chamber did not show an increase in hopping during the mating chorus, suggesting that a longer acclimation period resulted in less behaviorally active females (Fig. 7). Finally, since it has been hypothesized that the laminar and magnocellular nuclei are sensory-motor integrators (Endepols and Walkowiak, 2001), we looked for correlations between the number of hops during the acoustic stimulus and *egr-1* or *fos* expression in the three divisions of the torus. We did so in brains collected at 0.5 h, since this is the observation period for which we detected increases in hopping, and we found no covariation (all $p>0.23$; data not shown), suggesting that the acoustic stimulation is more important for induction of IEG expression in the torus than acoustically evoked locomotion. However, it is always possible that a relationship would emerge if we examined the effect of acoustically induced locomotion on IEG expression after a 1-h survival time. Nevertheless, if the motor response to the mating chorus was a significant component of the IEG response in the torus, we would not expect females acclimated for 24 h to show IEG responses similar to that of females acclimated for 6 h. This further suggests that IEG expression in the torus is driven primarily by acoustic input rather than motor output, although other aspects of locomotion we did not measure, such as orientation, may be important.

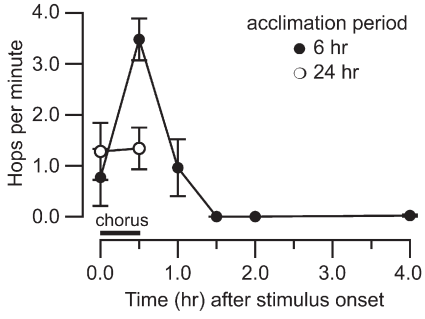

Fig. 7 – Locomotion (mean ± SE hops per minute) during the prior 30 min of females acclimated to the experimental chamber for 6 or 24 h before presentation of the mating chorus.

3. Discussion

We found robust acoustic activation of the immediate early genes (IEGs) *egr-1* and *fos* in the auditory midbrain of the túngara frog. Like other vertebrates, we found that sensory-induced IEG expression began to increase within 15–30 min after stimulus onset and began to decline within 30 min of acoustic isolation. Unlike in other vertebrates, however, in the túngara frog it took longer to reach the highest and lowest levels of mRNA in response to sound and isolation, respectively. We also found that the magnitude of acoustic induction of IEGs differed among the three subdivisions of the torus. Finally, although females increased locomotion in response to the mating chorus, we found no evidence that IEG mRNA levels in the torus were influenced by this motor response, which is consistent with a recent study on male túngara frogs (Hoke et al., 2007). Our results demonstrate the generality of sensory-induced IEG expression in vertebrates but raise the possibility of significant species variation in the temporal regulation of IEG mRNA.

The anuran torus semicircularis is an important site for the acoustic feature detection that is necessary for recognition and discrimination of mating calls (Endepols et al., 2003; Hall, 1994). In spite of significant progress in understanding the encoding of acoustic features by individual neurons in the torus (e.g., Edwards et al., 2002), the relative contributions of the three subdivisions to auditory processing remain less clear. Differences in anatomy and physiology of the three nuclei (Endepols and Walkowiak, 2001; Endepols et al., 2000) strongly suggest that they make distinct contributions to

auditory processing, but what exactly those contributions are is yet to be unequivocally demonstrated. The increased spatial resolution offered by IEG mapping approaches may provide an important advantage in deciphering the different functional roles of the three nuclei of the torus. For example, a previous study on male túngara frogs found that the laminar nucleus, but not the principal nucleus, showed acoustically induced variation in *egr-1* expression (Hoke et al., 2004). In particular, the laminar nucleus showed greater responses to signals of greater behavioral salience (Hoke et al., 2004). Our study extends this earlier work by examining temporal dynamics of IEG expression in the female torus, including an additional nucleus (the magnocellular nucleus) and an additional gene (*fos*). We found significant increases in both IEGs in all nuclei in response to acoustic stimulation, and, when we compared among the three nuclei, we found that acoustically induced *egr-1* expression was greatest for the principal nucleus. The greater *egr-1* response of the principal nucleus of females in our study compared to males in the study by Hoke et al. (2004) suggests an important sex difference in the auditory response to mating calls. Future studies of the relative IEG response to variation in mating call types in females may provide new clues to the relative contributions of the three subdivisions to auditory processing within a mate-choice context.

We were surprised that the time course of IEG mRNA expression in the túngara frog was substantially slower than the 30-min peak that is most often reported in other vertebrates. The apparent difference in IEG time course could be a result of differences in experimental design, which almost always varies among studies. However, the studies that are most similar to our own find that a 30-min presentation of song results in peak expression of *egr-1* and *fos* mRNA after a 30-min survival time (Mello and Clayton, 1994; Velho et al., 2005), suggesting that túngara frogs do indeed differ from zebra finches in the kinetics of IEG mRNA expression. Alternatively, it is possible that frogs are similar to other vertebrates in IEG kinetics, but the differences among studies are a consequence of the brain regions analyzed. Indeed, kinetics of IEG gene expression sometimes vary among brain regions (Kelly and Deadwyler, 2003). Whereas we measured IEG responses in the anuran homolog of the inferior colliculus, studies of the temporal dynamics of sensory-induced IEG expression in zebra finches and rats have focused on sensory regions of the telencephalon (Mello and Clayton, 1994; Velho et al., 2005; Zangenehpour and Chaudhuri, 2002). We are unaware of any reports of IEG expression time courses in the avian or mammalian inferior colliculus, and, unfortunately, no known homolog to sensory telencephalon of amniotes exists in anurans for comparison (Butler and Hodos, 2005). A third possibility is that the túngara frog differs from zebra finches and rats because frogs are ectotherms. Ectothermy, *per se*, is unlikely to explain our results since a teleost fish, also an ectotherm, showed a 30-min peak at an ambient temperature similar to that of this study (Burmeister and Fernald, 2005). However, since the relationship between metabolic physiology and kinetics of gene expression is largely unknown, a potential role of ectothermy cannot be excluded. Although further studies are clearly required to clarify these issues, the results of our study do raise the possibility of significant variation in the temporal kinetics of IEG mRNA expression among vertebrates. Our results also suggest that establishing a time course of IEG expression can be an important step when using IEG activity mapping in new species.

Although *egr-1* and *fos* had similar temporal kinetics, we found that the induction pattern for the two genes differed among brain regions. Furthermore, the lack of correlation between *egr-1* and *fos* mRNA levels within brain regions suggests that the two genes are largely independent of one another in terms of the magnitude of their mRNA expression levels in response to sound. In birds, the induction pattern of the two proteins vary with prior experience (Sockman et al., 2005) and with the sex of the individual (Bailey and Wade, 2003). This independent modulation of *egr-1* and *fos* expression is particularly interesting in light of recent findings that the two genes are almost exclusively expressed in the same neurons in the auditory telencephalon of zebra finches (Velho et al., 2005). Although we still have a lot to learn about the relative independence of *egr-1* and *fos* in the anuran auditory midbrain, our results suggest that, as in birds, the two genes could provide different information when used in IEG mapping studies.

The practical implications of our study for IEG activity mapping in the túngara frog are clear. First, although it is feasible to work with gravid females acclimated for less than 24 h, the longer acclimation period has the advantage of reducing the behavioral responses of the females. This is an advantage because it increases the specificity of the stimulus situation by eliminating confounding locomotor responses. Alternatively, if the question of interest includes locomotor responses (e.g., Hoke et al., 2007) it may be desirable to design experiments with shorter acclimation periods, as long as acclimation periods are at least 2 h, which is necessary to reach low levels of IEGs, and variation in locomotor responses is measured and accounted for. Second, our results indicate that future IEG mapping experiments in the túngara frog might benefit from a survival time of 1 h following stimulus onset. The 1-h group was the only group for which a difference between no sound and acoustic stimulation was detected for both genes in all brain regions, although most regions responded earlier. As a result, we presume that the 1-h time point is the most reliable for detecting differences among acoustic treatments and will, therefore, provide increased sensitivity when examining responses to variation in stimulus parameters (e.g., different mating calls). Of course, the generalizability of our results to other stimulus conditions awaits further studies. For example, we do not know whether a 1-h peak depends on a 30-min stimulus followed by 30 min of no sound or if shorter and longer stimuli will elicit similar patterns of IEG expression as has been found in zebra finch (Kruse et al., 2000). Finally, although further work needs to be done to determine the extent to which our results are representative of other frogs and toads, we hope that our study will generate increased interest in the use of IEG mapping in this and other anuran species. The barriers to using this approach are relatively few and the advantages are substantial. IEG activity mapping is particularly valuable for neuroethological model systems because it allows simultaneous assessment of neural activity of multiple brain regions in animals that were awake and free moving.

4. Experimental procedures

4.1. *Isolation of túngara specific egr-1 and fos probes*

Since our *P. pustulosus*-specific *egr-1* cDNA subclone had been previously reported (GenBank No. AY562993; Hoke et al., 2004), but no sequence analysis had been performed, we first verified the identity of our *P. pustulosus egr-1* subclone by comparing to sequences for *X. tropicalis*, chicken, and mouse. To identify the cDNA sequence for *P. pustulosus fos*, we used a combination of degenerate PCR and Rapid Amplification of cDNA Ends (RACE). We extracted RNA from brains using Trizol and synthesized cDNA using an anchored poly-dT primer and Superscript II reverse transcriptase (Invitrogen, Carlsbad, CA). For the degenerate PCR, we combined a forward primer (5′-CCT TCG TCC CCA CCG TNA CNG CNA T-3′) generated by Codehop (Rose et al., 1998) with a reverse primer (5′-GCY TCI GGR TAI GTR AAI AC-3′) previously described (Matsuoka et al., 1998). We amplified an 838-bp fragment using the following PCR cycling parameters: 2 min at 94 °C followed by 38 cycles of 1 min at 94 °C, 2 min at 50 °C, 3 min at 72 °C, and concluding with a final elongation of 72 °C for 7 min. We gel extracted a band of the anticipated size and reamplified using the following cycling parameters before sequencing: 2 min at 94 °C followed by 25 cycles of 1 min at 94 °C, 2 min at 55 °C, 3 min at 72 °C, and concluding with a final elongation of 72 °C for 7 min. We then designed the following gene-specific primers to amplify the 5′ and 3′ ends using SmartRACE (Clontech, Palo Alto, CA): forward, 5′-ATC ACA CCA GAG CGG CTG TAG GTT G-3′ and reverse, 5′-ATC TGA TGC TGC CCG TTC TGT ACC A-3′. We used cycling parameters as recommended by the SmartRACE protocol for total RNA starting material. We then assembled a full-length contiguous sequence and compared it to *fos* sequences for *X. tropicalis*, chicken, and mouse in GenBank.

4.2. *Decline in gene expression following isolation*

Many IEG studies use laboratory reared animals that are well acclimated to the experimental situation (typically 24–48 h). In the present study, we worked with wild-caught females who were captured while in a mating clasp ("amplexus") with a male at a mating chorus. We chose to work with mating females because the females' responses to acoustic stimuli vary with their reproductive stage and are at their maximum at the time of mating (Lynch et al., 2005). Females caught during this physiological stage typically release their eggs within 24 h, even in the absence of a male, and will subsequently be behaviorally unresponsive to acoustic stimuli (Lynch et al., 2005). Because of this constraint, we anticipate that future IEG studies with similar females will benefit by limiting the acclimation period to less than 24 h. Therefore, we first asked how long it takes for IEG expression to decline to stable low levels following acoustic isolation. In addition, for comparison, we included some brains collected immediately after capture at the breeding ponds.

Over a 3-week period, we caught females in amplexus at breeding ponds near Gamboa, Panama, between 19:58 and 22:18. The male was removed from the female and the female was placed into inflated plastic collection bags with a moist paper towel. Six females were decapitated at the breeding pond and all others were transported back to the Smithsonian Tropical Research Institute (STRI) laboratory which was maintained at ambient temperatures (about 28 °C). Four females were decapitated after returning to the laboratory (mean ± SD = 46.8 ± 15.2 min after capture) to represent gene expression levels before isolation (0-h time point). All other females in their plastic bags were placed into sound attenuation chambers and left in the quiet for 0.5, 1, 2, 4, 6, or 24 h (samples sizes were 4 for each group, except for the 24-h group which was 6). Among the 6 females who were in the boxes for 24 h, three released their eggs sometime during the 24-h period. See Fig. 2 for a time line of the experiment. We interspersed treatment groups (isolation time) across days; however, treatment groups were not fully interspersed across different times of the night. As a result, isolation time is somewhat confounded with absolute time of the night. At the end of the isolation period, we decapitated females, removed extraneous tissue from the head, immersed the heads in embedding medium (Tissue Tek OCT, Sakura Finetek, Torrance, CA), and froze the tissue in liquid nitrogen. We stored the tissue in liquid nitrogen until transportation to our UNC laboratory on dry ice and then stored the brains at −80 °C until sectioning. The Institute for Animal Care and Use Committee at the University of North Carolina approved all animal procedures and Panama's National Authority for the Environment (Autoridad Nacional del Ambiente) permitted our work in Panama.

We sectioned brains in the transverse plane at 12 μm in 4 series on a cryostat. To localize *egr-1* and *fos* gene expression, we used a radioactive *in situ* hybridization procedure, which results in deposition of silver grains in areas of riboprobe binding. The *egr-1* probes corresponded to nucleotides 1–309 of a 411-bp subclone. The *fos* probes were synthesized from a 1029-bp subclone corresponding to nucleotides 242–1270 of the full-length cDNA. We followed a similar protocol as in Hoke et al. (2004) with the following exceptions: we fixed the brain sections in 4% paraformaldehyde for 3 min followed by a wash in phosphate-buffered saline, we hybridized the tissue with 3×10^6 cpm/ml of hybridization buffer resulting in approximately 2.7×10^5 cpm per slide, and we included a room temperature wash in 0.1× SSC before dehydration and clearing in xylenes. We visualized the bound riboprobe as silver grains by exposing the slides to NTB emulsion (Kodak, New Haven, CT) for 8 days at 4 °C, and we visualized the cell bodies by staining the tissue with thionin. In all our *in situ* hybridization procedures, we always included sense probes and in no case did the sense probe result in binding.

To determine the effects of acoustic isolation on *egr-1* and *fos* mRNA expression in the brain, we quantified the number of silver grains above background per cell body in the laminar nucleus of the torus semicircularis. We restricted our analysis to the laminar nucleus in this first experiment because poor section quality prevented us from reliably sampling the principal and magnocellular nuclei. To sample the laminar nucleus, we quantified silver grains per cell at a magnification of 1000× of one hemisphere of the brain. The hemisphere was chosen at random except when one side of the brain was damaged, in which case the undamaged side was chosen. We calculated an individual's mean number of silver grains per cell from 1–4 sections (mean = 3.3 sections per frog) that were spaced 96 μm apart on average. We placed our sampling window (140 μm ×

100 μm) in the lateral portion of the laminar nucleus where the laminar arrangement of cells is particularly evident (Fig. 1).

For each brain section, we took three images: a color image of thionin-stained tissue in the area of interest, a blue-filtered image of the silver grains in the same field of view ("grains image"), and a blue-filtered image of a nearby area of the slide containing no tissue to represent local background silver grain density due to variation in emulsion thickness ("background image"). In the blue-filtered images, exposure time, brightness, and contrast settings were the same for each brain section of an individual subject, although these parameters varied slightly from section to section due to variation in darkness of thionin staining. We used Image J (National Institutes of Health, Bethesda, MD) to convert the grains and background images to black and white images using the 'make binary' function and to count the silver grains in each image using the 'analyze particles' function. We subtracted the number of background silver grains from the number of silver grains over the area of interest; consequently, our results represent only the silver grains above background levels. We also counted the number of cell bodies in the area of interest from the color image to represent relative mRNA expression levels as the number of silver grains above background per cell. Typically, high levels of *egr-1* or *fos* expression were seen in a subset of the cells being sampled and because we corrected the silver grain number by the number of all cells in the field of view, including those with no associated silver grains, the resulting number of silver grains per cell tends to be low.

In general, we used analysis of variance (ANOVA) with type III sums of squares and Fisher's least significant difference post hoc analyses. To examine the effect of isolation on IEG expression, we used an ANOVA with time of isolation and gene as factors and included all animals transported back to the STRI laboratory. In our analysis, we were interested in exploring differences between *egr-1* and *fos* in addition to the effect of isolation. However, we could not make direct comparisons between *egr-1* and *fos* because of differences in the *in situ* hybridization procedures (e.g., different probe lengths, *in situ* run at different times) and, as a consequence, we did not examine the effect of gene in our ANOVAs. Instead, we used interaction effects to investigate the differential responses of *egr-1* and *fos*. Interpreting the interaction terms does not depend on absolute differences between *egr-1* and *fos*. For example, the interaction between isolation time and gene will reveal whether the pattern of mRNA decline differed for *egr-1* and *fos* in which case the absolute differences in silver grain number between *egr-1* and *fos* are not important.

4.3. *Acoustically evoked gene expression*

We captured females at the ponds over a 2-week period and transported them back to the STRI laboratories as in our acoustic isolation experiment (described in Section 4.2). We modified the enclosure used by removing females from the collection bag and placing them in a perforated circular arena within the sound attenuation chambers for either 6 or 24 h in silence. Only females who kept their eggs for the duration of the experiment were included in the experiment. We then presented females with a 30-min stimulus that was created by looping a 15-min recording of a natural breeding chorus once. For females that experienced 6 h of acclimation, we collected their brains after survival times of 0, 0.25, 0.5, 0.75, 1, 1.5, 2, or 4 h after stimulus onset (sample size was 5 for each group). For females exposed to 24 h of acclimation, we collected their brains after 0 or 0.5 h after stimulus onset ($n=5$ for each group). See Fig. 2 for a time line of the experiment. To decouple absolute time from the experimental treatment groups, we interspersed groups (survival time after stimulus onset) across days of the experiment and across different times of the night. This interspersal ensured that any effect of survival time on IEG expression could not be attributed to an endogenous rhythm. Because acoustically guided locomotion is an important component of female mate choice in frogs, we recorded video of a subset of females ($n=36$) the last 30 min before decapitation and used the videos to count the number of hops the females produced per minute; we excluded females in the 0.25- and 0.75-h groups from the behavioral analysis since they were exposed to two different stimulus periods (e.g., no sound followed by sound) during the last 0.5 h before sacrifice. Brains were collected and stored as described above (see 4.2).

To improve our tissue quality, we sectioned brains at 16 μm in 3 series. We followed the same *in situ* hybridization protocol described above (see 4.2), although we exposed slides to NTB emulsion for 14 days at 4 °C before staining. Improved section quality allowed us to sample more sections from each brain region. As described above (see 4.2), we quantified the number of silver grains per cell body. Fig. 1 shows examples of sampling locations for each nucleus. For the laminar nucleus, we calculated the mean silver grains per cell from 2–4 sections (mean = 3.6 sections per frog) spaced 48 μm apart. For the principal nucleus, we calculated the mean silver grains per cell from 2–4 sections (mean = 3.7 sections per frog) spaced 48 μm apart. For the magnocellular nucleus, we calculated the mean silver grains per cell from 1–4 sections (mean = 3.3 sections per frog) spaced 48 μm apart.

To assess the effect of acclimation period on acoustically induced IEG expression, we restricted our analysis to females decapitated at 0 or 0.5 h following stimulation since these are the only time points for which we had groups acclimated for 6 and 24 h; for these analyses we looked for two-way interactions between acclimation period and survival time (acclimation × survival time), and we conducted separate ANOVAs for each gene and brain region. To test whether survival time following stimulus onset influenced IEG expression more generally, we conducted a four-way ANOVA with survival time, gene, brain region, acclimation period, and their interactions as factors. Since our primary interest was in the acoustic stimulation of *egr-1* and *fos* and not, for example, the subsequent decline, we followed-up this ANOVA with analyses including animals only in the 0- and 1-h groups; we chose 1 h because we observed maximum mRNA levels at this time point (see Section 2.3). In addition, as described above (see 4.2), we tested for effects of gene by examining interactions between gene and other factors in our analyses.

Acknowledgments

We gratefully acknowledge assistance from Dr. Michael J. Ryan in carrying out the experiments. We also thank Ms. Ellie

Kemple for her assistance in the field, Ms. Mukta Chakraborty for her contributions to cloning *fos*, Mr. Tyler Martin for his contributions to the behavioral quantification, the staff at the Smithsonian Tropical Research Institute for their logistical support in Panama, and Dr. Keith W. Sockman for use of his laboratory equipment. This work was funded in part by NSF 0445682 to S.S.B.

REFERENCES

Bailey, D.J., Wade, J., 2003. Differential expression of the immediate early genes *FOS* and *ZENK* following auditory stimulation in the juvenile male and female zebra finch. Mol. Brain Res. 116, 147–154.

Burmeister, S.S., Fernald, R.D., 2005. Evolutionary conservation of the *egr-1* immediate-early gene response in a teleost. J. Comp. Neurol. 481, 220–232.

Butler, A.B., Hodos, W., 2005. Comparative Vertebrate Neuroanatomy: Evolution and Adaptation, 2nd edn. Wiley-Liss, Hoboken. 744 pp.

Clayton, D.F., 2000. The genomic action potential. Neurobiol. Learn. Mem. 74, 185–216.

Edwards, C.J., Alder, T.B., Rose, G.J., 2002. Auditory midbrain neurons that count. Nat. Neurosci. 5, 934–936.

Endepols, H., Walkowiak, W., 2001. Integration of ascending and descending inputs in the auditory midbrain of anurans. J. Comp. Physiol., A Sens. Neural Behav. Physiol. 186, 1119–1133.

Endepols, H., Walkowiak, W., Luksch, H., 2000. Chemoarchitecture of the anuran auditory midbrain. Brain Res. Rev. 33, 179–198.

Endepols, H., Feng, A.S., Gerhardt, H.C., Schul, J., Walkowiak, W., 2003. Roles of the auditory midbrain and thalamus in selective phonotaxis in female gray treefrogs (*Hyla versicolor*). Behav. Brain Res. 145, 63–77.

Feng, A.S., Lin, W.Y., 1991. Differential innervation patterns of three divisions of frog auditory midbrain (torus semicircularis). J. Comp. Neurol. 306, 613–630.

Gerhardt, H.C., Huber, F., 2002. Acoustic Communication in Insects and Anurans. University of Chicago Press, Chicago. 542 pp.

Hall, J., 1994. Central processing of communication sounds in the anuran auditory system. Am. Zool. 34, 670–684.

Hoke, K.L., Burmeister, S.S., Fernald, R.D., Rand, A.S., Ryan, M.J., Wilczynski, W., 2004. Functional mapping of the auditory midbrain during mate call reception. J. Neurosci. 24, 11264–11272.

Hoke, K.L., Ryan, M.J., Wilczynski, W., 2005. Social cues shift functional connectivity in the hypothalamus. Proc. Natl. Acad. Sci. U. S. A. 102, 10712–10717.

Hoke, K.L., Ryan, M.J., Wilczynski, W., 2007. Integration of sensory and motor processing underlying social behaviour in túngara frogs. Proc. R. Soc. Lond., B 274, 641–649.

Honkaniemi, J., Kononen, J., Kainu, T., Pyykonen, I., Pelto-Huikko, M., 1994. Induction of multiple immediate early genes in rat hypothalamic paraventricular nucleus after stress. Mol. Brain Res. 25, 234–241.

Honkaniemi, J., Sagar, S.M., Pyykonen, I., Hicks, K.J., Sharp, F.R., 1995. Focal brain injury induces multiple immediate early genes encoding zinc finger transcription factors. Mol. Brain Res. 28, 157–163.

Jarvis, E.D., 2004. Learned birdsong and the neurobiology of human language. Ann. N.Y. Acad. Sci. 1016, 749–777.

Jarvis, E.D., Scharff, C., Grossman, M.R., Ramos, J.A., Nottebohm, F., 1998. For whom the bird sings: context-dependent gene expression. Neuron 21, 775–788.

Keefe, K.A., Gerfen, C.R., 1999. Local infusion of the (+/–)-alpha-amino-3-hydroxy-5-methylisoxazole-4-propionate/kainate receptor antagonist 6-cyano-7-nitroquinoxaline-2, 3-dione does not block D1 dopamine receptor-mediated increases in immediate early gene expression in the dopamine-depleted striatum. Neuroscience 89, 491–504.

Kelly, M.P., Deadwyler, S.A., 2003. Experience-dependent regulation of the immediate-early gene arc differs across brain regions. J. Neurosci. 23, 6443–6451.

Kruse, A.A., Stripling, R., Clayton, D.F., 2000. Minimal experience required for immediate-early gene induction in zebra finch neostriatum. Neurobiol. Learn. Mem. 74, 179–184.

Lynch, K.S., Rand, A.S., Ryan, M.J., Wilczynski, W., 2005. Plasticity in female mate choice associated with changing reproductive states. Anim. Behav. 69, 689–699.

Matsuoka, I., Fuyuki, K., Shoji, T., Kurihara, K., 1998. Identification of c-*fos* related genes and their induction by neural activation in rainbow trout brain. Biochim. Biophys. Acta 1395, 220–227.

Mello, C.V., 2004. Gene regulation by song in the auditory telencephalon of songbirds. Front. Biosci. 9, 63–73.

Mello, C.V., Clayton, D.F., 1994. Song-induced *ZENK* gene expression in auditory pathways of songbird brain and its relation to the song control system. J. Comp. Neurol. 14, 6652–6666.

Mello, C., Nottebohm, F., Clayton, D., 1995. Repeated exposure to one song leads to a rapid and persistent decline in an immediate early gene's response to that song in zebra finch telencephalon. J. Neurosci. 15, 6919–6925.

Park, K.H., Clayton, D.F., 2002. Influence of restraint and acute isolation on the selectivity of the adult zebra finch *zenk* gene response to acoustic stimuli. Behav. Brain Res. 136, 185–191.

Potter, H.D., 1965. Mesencephalic auditory region of the bullfrog. J. Neurophysiol. 28, 1132–1154.

Rose, T.M., Schultz, E.R., Henikoff, J.G., Pietrokovski, S., McCallum, C.M., Henikoff, S., 1998. Consensus-degenerate hybrid oligonucleotide primers for amplification of distantly related sequences. Nucleic Acids Res. 26, 1628–1635.

Ryan, M.J., 2005. The evolution of behaviour, and integrating it towards a complete and correct understanding of behavioural biology. Anim. Biol. 55, 419–439.

Sockman, K.W., Gentner, T.Q., Ball, G.F., 2002. Recent experience modulates forebrain gene-expression in response to mate-choice cues in European starlings. Proc. R. Soc. Lond., B 269, 2479–2485.

Sockman, K.W., Gentner, T.Q., Ball, G.F., 2005. Complementary neural systems for the experience-dependent integration of mate-choice cues in the European starling. J. Neurobiol. 62, 72–81.

Thiriet, N., Zwiller, J., Ali, S.F., 2001. Induction of the immediate early genes *egr-1* and c-*fos* by methamphetamine in mouse brain. Brain Res. 919, 31–40.

Velho, T.A., Pinaud, R., Rodrigues, P.V., Mello, C.V., 2005. Co-induction of activity-dependent genes in songbirds. Eur. J. Neurosci. 22, 1667–1678.

Wilczynski, W., Rand, A.S., Ryan, M.J., 2001. Evolution of calls and auditory tuning in the *Physalaemus pustulosus* species group. Brain Behav. Evol. 58, 137–151.

Zangenehpour, S., Chaudhuri, A., 2002. Differential induction and decay curves of c-fos and zif268 revealed through dual activity maps. Mol. Brain Res. 109, 221–225.